IEEE Access
Multidisciplinary | Rapid Review | Open Access Journal

Received October 20, 2021, accepted November 1, 2021, date of publication November 4, 2021, date of current version November 16, 2021.

Digital Object Identifier 10.1109/ACCESS.2021.3125316

Composite Speed Control of PMSM Drive System Based on Finite Time Sliding Mode Observer

WEI XU[1], (Senior Member, IEEE), ABDUL KHALIQUE JUNEJO[1,2], YIRONG TANG[1], (Student Member, IEEE), MUHAMMAD SHAHAB[1], HABIB UR RAHMAN HABIB[3], (Graduate Student Member, IEEE), YI LIU[1], (Senior Member, IEEE), AND SHOUDAO HUANG[4], (Senior Member, IEEE)

[1]State Key Laboratory of Advanced Electromagnetic Engineering and Technology, Huazhong University of Science and Technology, Wuhan 430074, China
[2]Department of Electrical Engineering, Qaid-e-Awam University of Engineering, Science and Technology, Nawabshah, Sindh 67450, Pakistan
[3]Department of Electrical Engineering, University of Engineering and Technology Taxila, Taxila 47050, Pakistan
[4]College of Electrical and Information Engineering, Hunan University, Changsha 410082, China

Corresponding author: Abdul Khalique Junejo (ak.junejo@gmail.com)

This work was supported in part by the National Natural Science Foundation of China under Grant 51877093, in part by the National Key Research and Development Program of China under Grant 2018YFE0100200, and in part by the Key Technical Innovation Program of Hubei Province under Grant 2019AAA026.

ABSTRACT The robust nonlinear speed control technique has been proposed for the speed regulation of permanent magnet synchronous motor (PMSM) by adopting a new fast terminal sliding mode control (FTSMC) based on the finite time sliding mode observer (FTSMO). The proposed technique can ensure the robustness against load disturbances, which has the capability of high tracking precision, fast finite time convergence and smooth dynamic operation in both transient and steady state conditions. Moreover, the requirement of high switching gain to reach the upper bound limit of total disturbances may produce the steady state error and chattering. To address this issue, one robust FTSMO based FTSMC is designed to alleviate those limitations aforementioned. The FTSMO can successfully estimate the total disturbances of the system, then the estimated disturbances can be compensated by the feed-forward compensation technique. The FTSMO based FTSMC should require the smaller switching gain to meet upper bound limit of the disturbances compared with the conventional SMC (CSMC) and FTSMC. The stability of the close loop control system is fully verified by the Lyapunov theory. Comprehensive simulation and experimental results have fully demonstrated that the proposed method is robust against load disturbances.

INDEX TERMS Permanent magnet synchronous motor (PMSM), sliding mode control (SMC), fast terminal sliding mode control (FTSMC), finite time sliding mode observer (FTSMO).

I. INTRODUCTION

Due to the high power and torque density, the permanent magnet synchronous motor (PMSM) has been applied in many emerging applications, such as electric vehicle (EV) [1]. The linear control algorithms have been widely employed in PMSM drive systems since they are easy to implement in practice [2]. As the practical PMSM system is nonlinear, time variant and complex with uncertainties, the linear algorithms may fail to attain the adequate performance in the whole operating range [3]. In order to increase the PMSM drive performance, great efforts in recent years have been made to develop nonlinear control techniques, such as adaptive control [4], disturbance rejection [5], [6], finite time control [7], linear sliding mode control (SMC) [8], robust control, predictive control [9], fuzzy and neural control [10], back stepping and intelligent control [1], [7], [10], and so on. These nonlinear control techniques are used to improve the drive performance from different application requirements.

Fortunately, the SMC techniques are found more effective to enhance the system robustness against load disturbances and uncertainties of PMSM drive systems [11]. However, the conventional SMC techniques can only improve the convergence rate of the system in the reaching time, but not in the sliding time. Thereof, the nonlinear terminal sliding mode (TSM) surface of the SMC is used to guarantee the system robustness, which can ensure the convergence in finite time at the reaching period and in sliding mode as well. The TSM

The associate editor coordinating the review of this manuscript and approving it for publication was Zheng Chen.

has the capability to improve the system convergence in finite time and robust against nonlinearities. The prominent drawback of nonlinear TSM is the chattering phenomena, which is brought by the discontinuous control law and periodic switching action near to the sliding surface. To alleviate the chattering phenomena in the SMC, different techniques are proposed as the saturation function instead of sign function, but the anti-disturbance performance has been compromised to some extent [12]. The selection of switching gain is a big issue in linear and TSM SMC techniques, which should choose one large value to reach the upper bound limit of disturbance and uncertainties. The chattering phenomenon would be produced in the control input due to the high value of the switching gain for the control law, as needed for the disturbance rejection process. The potential disadvantage of high switching gain can be solved by the full order SMC [13] and continuous terminal SMC [14].

In this paper, a new fast terminal SMC (FTSMC) has been adapted for the PMSM drive system, which has the capability of fast finite time convergence, high tracking precision, excellent steady state process, and effective chattering alleviation in the whole system. The problem of the high switching gain selection can be solved through the implementation of the observers in the close loop system. The disturbances can be estimated by the observers, then the estimated disturbances would be brought for the feed forward compensation method of the close loop system. The adaptive SMC is used to estimate the disturbances for the position control [15]–[17]. Many other techniques have been used to estimate the nonlinearities for compensation, e.g. the extended state observer based on the SMC.

Due to the stunning performance, the FTSMC is designed in this paper for its fast finite time convergence and robust against nonlinearities in the sliding trajectory. It is observed that the high value of switching gain in the control law is needed to meet the upper bound limit of the disturbances of the control system, the chattering would be induced in the control input due to the requirement of the high switching gains for control law. Consequently, due to that one estimation process is needed to alleviate the aforementioned problems in the system, the total or partial estimation technique of the disturbances can reduce the switching gain in the control law, which would alleviate the chattering of the whole system.

Hence, in this paper, one improved FTSMO based FTSMC is proposed to solve the defects of conventional methods. The FTSMO can estimate the total disturbance of the system, in which the estimated disturbances are compensated by the feed-forward compensation technique. The proposed technique can alleviate the chattering phenomena in the system effectively. This paper is organized by six sections. In Section I, the relevant literature review is fully made. The dynamic modeling of the PMSM is presented in Section II. The speed controller is designed by FTSMC, which is represented in Section III. In Section IV, the FTSMO is designed to estimate the disturbances of the system for feed-forward compensation process. Comprehensive simulation and experimental results are given out in Section V, which have fully confirmed that the FTSMO can get stronger anti-disturbances ability, greater robust capability, faster convergence speed, and so on. Finally, conclusions have been drawn in Section VI.

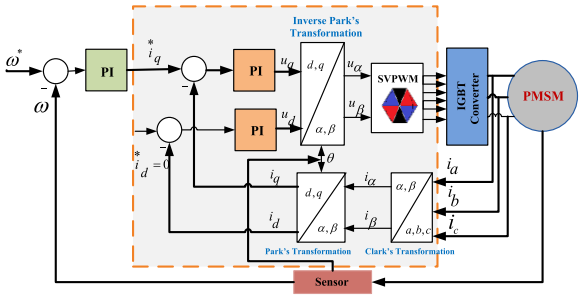

FIGURE 1. Diagram of the PMSM drive under the FOC control.

II. MODELLING OF THE PMSM DRIVE SYSTEM

The PMSM dynamic model can be obtained with the help of the synchronous reference frame. The speed and dynamic dq-axis currents can be described as

$$J\frac{d\omega}{dt} = X_t i_q - B\omega - n_p T_L \tag{1}$$

$$L_s\frac{di_d}{dt} = -Rsi_d + L_s n_p \omega i_q + u_d \tag{2}$$

$$L_s\frac{di_q}{dt} = -Rsi_q + L_s n_p \omega i_d - n_p \omega \psi_f + u_q \tag{3}$$

where $X_{\mathrm{t}} = 3/2\ n_p^2 \psi_{\mathrm{f}}$, $F_t = X_t\ /J$, n_p is the number of pole pairs, ψ_f the flux linkage, J the moment of inertia, B the viscous damping co-efficient, and u_d, u_q, i_d and i_q are the d- and q- axis voltages and currents, respectively, R_{s} and L_{s} the resistance and inductance of the stator, respectively, ω is the mechanical angular speed, and T_L the load torque.

In this paper, the speed loop is considered with load disturbances, hence the speed equation with disturbances can be written as

$$\dot{\omega} = F_t i_q + y_\omega(t) \tag{4}$$

where $y_\omega(t) = -\frac{B}{J}\omega - \frac{n_p}{J}T_L$ is the total disturbances for the drive system. The simple diagram of field-oriented control (FOC) for the PMSM is shown in Fig. 1, which contains two main loops (one for the speed and another for the current loop), respectively. In order to decouple the speed and current loops, it is supposed $i_d = 0$, and the PI based current controllers are adopted to stabilize the current dynamics in dq-axis for current loops, separately. In this paper, the speed loop has been designed for the speed regulation.

III. DESIGN OF THE SPEED CONTROLLER

A. THE DESIGN OF THE SPEED LOOP CONTROLLER UNDER THE FTSMC

In this work, the actual and reference speeds of the PMSM are ω and ω^*, respectively. The speed error E can be described as

$$\mathrm{E} = \omega^* - \omega \tag{5}$$

Taking the derivation of (5) and combining with (4), it will get the mathematical expression on $\dot{\mathrm{E}}$ by

$$\dot{\mathrm{E}} = \dot{\omega}^* - F_t i_q - y_\omega(t) \tag{6}$$

In general, the conventional sliding surface can be described as

$$\vartheta = \dot{\mathrm{E}} + \mu \times \mathrm{E}, \quad \mu > 0 \tag{7}$$

The working process takes much longer time to reach the steady state operation, which means that the state would not converge quickly under the steady state and transient conditions by the conventional SMC. Therefore, some TSMC techniques have been used to resolve the problem of chattering and convergence. Particularly, the TSMC [18] and non-singular terminal SMC (NTSMC) [19] can be described as

$$\vartheta = \dot{\mathrm{E}} + \mu \times \mathrm{E}^{\delta}, \quad \mu > 0,\ 0 < \mu < 1 \tag{8}$$

$$\vartheta = \mathrm{E} + \mu \times \dot{\mathrm{E}}^{\delta'}, \quad \mu' > 0,\ 0 < \mu' < 1 \tag{9}$$

It can be noted that (7) would be the same as (8) when $\delta = 1$, due to $0 < \delta < 1$, δ can be selected as $\delta = q/p$, where q and p are the positive odd integers, and likewise δ' is adopted as $u = q/p$, respectively. Furthermore, the NTSMC has the slow convergence rate when the states are far away from the equilibrium point [19]. Moreover, to enhance the convergence of the system states, one new FTSMC has been proposed in this paper, which has the capability of high tacking precision, fast convergence and robust against load disturbances. The new FTSMC technique is illustrated as

$$\vartheta = \dot{\mathrm{E}} + \mu_1 \left|\dot{\mathrm{E}}\right|^{\sigma_1} sign\left(\dot{\mathrm{E}}\right) + \mu_2 \left|\mathrm{E}\right|^{\sigma_2} sign\left(\mathrm{E}\right) \tag{10}$$

where coefficients $\mu_1 > 0$, $\mu_2 > 0$, $0 < \sigma_1 < 2$, $\sigma_2 > \sigma_1$, and $\sigma_1 = t/u$, both t and u are the odd positive number. One novel terminal sliding reaching law (TSRL) type is employed to enhance the speed response of motor system in transient process and reduce the chattering phenomenon [20]. The TSRL can be illustrated as

$$\dot{\vartheta} = -\lambda_1(\vartheta) - \lambda_2 \left|\vartheta\right|^{\delta_3} sign(\vartheta) \tag{11}$$

where λ_1, λ_2 and δ_3 are carefully designed for the robustness of speed control loop under speed and load change. The λ_1 and λ_2 are positive constants and the value of $\delta 3$ is bounded as $0 < \delta_3 < 1$.

Statement 1. The speed error in (5) is chosen as state variable for the design of the speed controller under FTSMC with TSRL of the PMSM drive system. The E can converge to the sliding mode surface (10) with TSRL (11) as $\vartheta = 0$. Therefore, the control law for the speed controller can be described as

$$i_q^* = F_t(H_{eq} + H_b) \tag{12}$$

$$H_{eq} = \dot{\omega}^* + \mu_1 \left|\dot{\mathrm{E}}\right|^{\sigma_1} sign\left(\dot{\mathrm{E}}\right) + \mu_2 \left|\mathrm{E}\right|^{\sigma_2} sign\left(\mathrm{E}\right) \tag{13}$$

$$H_b = \int_0^t \lambda_1(\vartheta) + \lambda_2 \left|\vartheta\right|^{\delta_3} sign(\vartheta) dt \tag{14}$$

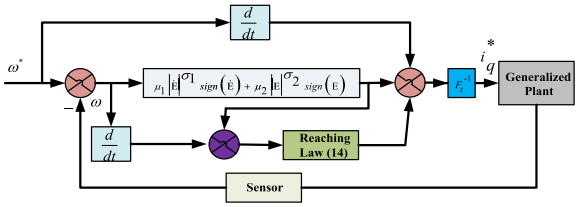

FIGURE 2. Block diagram of the sliding mode speed controller based on the FTSMC.

The block diagram of the sliding mode speed controller based on the FTSMC is shown in Fig.2. Some assumption and statement are given out and discussed as follows.

Assumption 1: Suppose the derivative of disturbance ($\dot{y}_\omega(t)$) is bounded, and there exists a constant $\xi_{y\omega} > 0$, such that $|\dot{y}_\omega(t)| \le \xi_{y\omega}$ is true for all $t \ge 0$, where $y_\omega(t)$ is the total disturbance of (4).

Statement 2: Assume the system (4) can satisfy the assumption 1 under the law from (12) to (14). The speed error will converge to zero at the sliding surface in the finite time, where the switching gain must satisfy the condition k2 > ξy ω.

The stability can be verified by the Lyapunov function, the According to (6) the (10) can be rewritten as

$$\begin{aligned}\vartheta &= \dot{\mathrm{E}} + \mu_1 \left|\dot{\mathrm{E}}\right|^{\sigma_1} sign\left(\dot{\mathrm{E}}\right) + \mu_2 \left|\mathrm{E}\right|^{\sigma_2} sign\left(\mathrm{E}\right) \\ &= \dot{\omega}^* - F_t i_q^* - y_\omega(t) + \mu_1 \left|\dot{\mathrm{E}}\right|^{\sigma_1} sign\left(\dot{\mathrm{E}}\right) \\ &\quad + \mu_2 \left|\mathrm{E}\right|^{\sigma_2} sign\left(\mathrm{E}\right). \end{aligned} \tag{15}$$

Substituting (12) - (14) into (15), the sliding mode surface can be derived as

$$\begin{aligned}\vartheta = \dot{\omega}^* - F_t[F_t^{-1}(H_{eq} + H_b)] - y_\omega(t) + \mu_1 \left|\dot{\mathrm{E}}\right|^{\sigma_1} sign\left(\dot{\mathrm{E}}\right) \\ + \mu_2 \left|\mathrm{E}\right|^{\sigma_2} sign\left(\mathrm{E}\right). \end{aligned} \tag{16}$$

Meanwhile, Eq. (16) can be simplified as

$$\vartheta = -H_b - y_\omega(t) \tag{17}$$

Then, the Lyapunov function is considered as (v = 1/2 ϑ_2) in this work. By taking derivative of (17) and combining with the error of PMSM system (6), it will get

$$\begin{aligned}\dot{\vartheta} &= -\dot{H}_b - \dot{y}_\omega(t) \\ &= -\lambda_1(\vartheta) - \lambda_2 \left|\vartheta\right|^{\sigma_3} sign(\vartheta) - \dot{y}_\omega(t). \end{aligned} \tag{18}$$

Hence, the following relationship can be obtained by

$$\dot{\vartheta}\vartheta = [-\lambda_1(\vartheta) - \lambda_2 \left|\vartheta\right|^{\delta_3} sign(\vartheta) - \dot{y}_\omega(t)]\vartheta \tag{19}$$

According to Statement 1, Eq. (19) can be rewritten as

$$\begin{aligned}\dot{V} &= \dot{\vartheta}\vartheta = -\lambda_1(\vartheta)^2 - \lambda_2 \left|\vartheta\right|^{\sigma_3+1} - \dot{y}_\omega(t)\vartheta \\ &\le -\lambda_1(\vartheta)^2 - \lambda_2 \left|\vartheta\right|^{\sigma_3+1} - \left|\dot{y}_\omega(t)\right| \left|\vartheta\right| \\ &\le -\lambda_1(\vartheta)^2 - \left[\lambda_2 + \frac{\left|\dot{y}_\omega(t)\right|}{\left|\vartheta\right|^{\sigma_3}}\right] \left|\vartheta\right|^{\sigma_3+1} \\ &\le -\lambda_1(\vartheta)^2 - \left[\lambda_2 + \xi_{y\omega}\right] \left|\vartheta\right|^{\sigma_3+1} \\ &= -2\tau_1 V - 2^{\frac{\sigma_3+1}{2}} \tau_2 V^{\frac{\sigma_3+1}{2}} \end{aligned} \tag{20}$$

where τ_1 and τ_2 are the positive constants. From (20), it is confirmed from (20) that the speed error of the controller would converge to zero in finite time when the inequality $\lambda_2 > \xi_{y\omega}$, and the finite time t_f, as expressed by

$$t_f = \int_0^{E(0)} \frac{\lambda_1^{1/\sigma_1}}{(E + \lambda_2 E^{\sigma_2})^{1/\sigma_2}} d\varepsilon = \frac{\lambda_1 |E(0)|^{1-1/\sigma_1}}{\lambda_2(\sigma_1 - 1)} \cdot R(\frac{1}{\sigma_1}; \frac{\sigma_1 - 1}{(\sigma_2 - 1)\sigma_1}; 1 + \frac{\sigma_1 - 1}{(\sigma_2 - 1)\sigma_1}; -\lambda_2 |E(0)|^{\sigma_2 - 1}) \quad (21)$$

where $R(\cdot)$ shows the Gauss Hyper-Geometric [21]. Meanwhile, Eq. (21) shows that the states would approach to the sliding surface in the finite time, i.e. getting convergence to zero gradually.

Remark 1: It can be noted that the gains λ_1 and λ_2 in the reaching law must be larger value to handle the effect of nonlinearities [21], [22]. The large switching gain value can produce the saturation problem in the drive system, while small values cannot ensure the finite time convergence and not good enough for the anti-disturbance. However, the FTSMO has been developed in this paper to estimate the nonlinearities in the system and compensate the system gains, which depends on the upper bound of estimation, as designed in the latter section regarding the FTSMO in details.

IV. OBSERVER DESIGN FOR THE ESTIMATION

A. ESTIMATION ON DISTURBANCES AND UNCERTAINTIES

It is known that the rejection ability of the load disturbances in CSMC is poorer than the FTSMC. Therefore, the FTSMC has been designed to improve the load disturbance rejection ability of the system. The FTSMC has the ability of fast convergence, high tracking precision and robust against the load disturbance. Furthermore, the estimation of the total disturbances is important for the composite controller to compensate the total disturbances. The feed forward compensation technique is used to reduce the system disturbances. Moreover, the FTSMO is employed for estimation of the system disturbances.

The FTSMO is adopted for the estimation of disturbances because the conventional disturbance observers have some limitations, i.e. the Luenberger observer brings the steady state error in the system, and then the sliding mode observer would produce the inherent chattering phenomenon in the system. Moreover, the high order differentiator (HOD) is designed and adopted for the numerical calculation. Then, the HOD is modified as the improved FTSMO in this paper for estimation on total disturbances of the PMSM drive system.

The FTSMO can be designed and implemented by considering a first order system $\dot{m} = f(m) + y(t)$, where m is the system state, and $y(t)$ the system disturbances. Then the FTSMO is written as

$$\begin{aligned} \dot{z}_o &= w_o + f(m) \\ w_o &= -\gamma_o k^{1/3} |z_o - m|^{2/3} sign(z_o - m) + z_1 \\ \dot{z}_1 &= w_1, \\ w_1 &= -\gamma_1 k^{1/2} |z_1 - w_o|^{2/3} sign(z_1 - w_o) + z_2 \\ \dot{z}_2 &= -\gamma_2 k sign(z_2 - w_1) \end{aligned} \quad (22)$$

where γ_o, γ_1, γ_2 and k are the observer co-efficients, z_o, z_1 and z_2 the observer variables, respectively. Therefore, z_1 can converge to $y(t)$ in the finite time with the proper selection of the FTSMO gains.

B. IMPROVED FTSMO DESIGNED FOR THE SPEED LOOP

The speed loop (4) has been modified according to the load disturbances of the system. One improved FTSMO has been implemented for the estimation of the system disturbances. Then, the FTSMO can be described by the feed-forward compensation technique, as illustrated by

$$\begin{aligned} \dot{\hat{\omega}} &= \frac{3}{2}\frac{n_p^2}{J}\psi_f i_q - \frac{B}{J}\hat{\omega} + w_o \\ w_o &= -\gamma_o k^{1/3} |\hat{\omega} - \omega|^{2/3} sign(\hat{\omega} - \omega) + \hat{y}_\omega(t) \\ \dot{\hat{y}}_\omega(t) &= w_1 \\ w_1 &= -\gamma_1 k^{1/2} |\hat{y}_\omega(t) - w_o|^{2/3} sign(\hat{y}_\omega(t) - w_o) + z_2 \\ \dot{z}_2 &= -\gamma_2 k sign(z_2 - w_1) \end{aligned} \quad (23)$$

where $\widehat{\dot{y}}_\omega(t)$ and $\dot{\hat{\omega}}$ are the estimated disturbances and speed derivation, γ_o, γ_1 and γ_2 the co-efficients of the FTSMO, w_o and w_1 different variables in the disturbances estimation process.

Remark 2: It is noted from the FTSMO that the proper selection of γ_o, γ_1, γ_2 and are very important in practice. The tracking performance indexes of the system would be affected by the unmolded dynamics, measuring noise, and limited control energy of the system. One reasonable switching gain can shorten the system convergence time effectively, while higher gain values of the FTSMO would result in the overshoot for the speed response. Therefore, it is required that the careful estimation on the total disturbances should be made for the compensation process.

Furthermore, it should be noted that the high gain values of σ_1 and σ_2 can improve the convergence of the close loop control system, which can induce the high chattering in the control input at the same time. Furthermore, σ_3 should be chosen properly because it would appear on the rejection ability of the load disturbances and chattering of the system. Hence, it is drawn that the parameters of the FTSMO based on FTSMC would influence the robustness capability of the system.

C. STABILITY ANALYSIS OF THE FTSMO

In this work, it is supposed that the FTSMO has differential inputs, and ω and i_q have the Lipschitz constant N >0 for their derivatives. From (4) and (23), the error variables of the observer can be described as $\ell_o = \hat{\omega} - \omega$, $\ell_1 = \hat{y}_\omega(t) - y_\omega(t)$, and $\ell_2 = \hat{\dot{y}}_\omega(t) - \dot{y}_\omega(t)$. Therefore, the observer errors can be

written as

$$\begin{aligned}\dot{\ell}_o &= -\frac{B}{J}(\ell_o) - \gamma_o k^{1/3} |\ell_o|^{2/3} sign(\ell_o) + \ell_1 \\ \dot{\ell}_1 &= -\gamma_1 k^{1/2} |\ell_1 - \dot{\ell}_o|^{1/2} sign(\ell_1 - \dot{\ell}_o) + \ell_2 \\ \dot{\ell}_2 &\in -\gamma_2 k sign(\ell_2 - \dot{\ell}_1) + [-N, N] \end{aligned} \tag{24}$$

The Lyapunov function has been used to check the stability of the FTSMO, and hence the satisfied conditions are described as

$$\begin{aligned} \nu_1 &= \frac{1}{2}\ell_o^2, \quad \dot{\nu}_1 = \ell_o.\dot{\ell}_o \le 0 \\ \nu_2 &= \frac{1}{2}\ell_1^2, \quad \dot{\nu}_2 = \ell_1.\dot{\ell}_1 \le 0 \\ \nu_3 &= \frac{1}{2}\ell_2^2, \quad \dot{\nu}_3 = \ell_2.\dot{\ell}_2 \le 0 \end{aligned} \tag{25}$$

The converging principle of the FTSMO can be expressed as $\hat{\omega} \to \omega, \hat{y}_\omega(t) \to y_\omega(t)$, and $z = \hat{y}_\omega(t) \to y_\omega(t)$. By taking the derivative of ν_1, which is the first Lyapunov function of (25), the derivative of ν_1 can be described as

$$\begin{aligned} \dot{\nu}_1 &= \ell_o.\dot{\ell}_o = \ell_o \left(-\frac{B}{J}(\ell_o) - \gamma_o k^{1/3} |\ell_o|^{2/3} sign(\ell_o) + \ell_1 \right) \\ &= \left(-\frac{B}{J}(\ell_o)^2 - \gamma_o k^{1/3} |\ell_o|^{5/3} + \ell_o.\ell_1 \right) \end{aligned} \tag{26}$$

It is seen that $\dot{\nu}_1 \le 0$ would satisfy the condition of Lyapunov function, when the proper selection of the γ_o and k has been achieved. Simultaneously, the $\dot{\ell}_o$ will converge to ℓ_1 and the two errors of (24) can be combined together, as illustrated by

$$\begin{aligned} \ell_1 - \dot{\ell}_o &= \frac{B}{J}(\ell_o) + \gamma_o k^{1/3} |\ell_o|^{2/3} sign(\ell_o) \\ \ell_2 - \dot{\ell}_1 &= \gamma_1 k^{1/2} |\ell_1 - \dot{\ell}_o|^{1/2} sign(\ell_1 - \dot{\ell}_o) \\ &= \gamma_1 k^{1/2} \left| -\frac{B}{J}(\ell_o) - \gamma_o k^{1/3} |\ell_o|^{2/3} sign(\ell_o) \right|^{1/2} \\ &\quad \times sign(\frac{B}{J}(\ell_o) \\ &\quad + \ell_o k^{1/3} |\ell_o|^{2/3} sign(\ell_o) \end{aligned} \tag{27}$$

Similarly, $\dot{\nu}_2 = \ell_1.\dot{\ell}_1 \le 0$ and $\dot{\nu}_3 = \ell_2.\dot{\ell}_2 \le 0$ would be satisfied by selecting the proper gains of γ_o, γ_1, γ_2 and k. In order to reach the requirement of (27), it should satisfy with the following condition by

$$\begin{aligned} \ell_o k^{1/3} &\ge -\frac{B}{J} |\ell_o|^{1/3} \pm \frac{\ell_1}{\ell_o^{2/3}} \\ \ell_1 k^{1/2} &\ge max \left(\frac{\ell_2}{|\ell_o|^{1/2}} \right) \\ \ell_2 k &\ge N \end{aligned} \tag{28}$$

Based on what mentioned above, it is concluded the design procedure of the FTSMO and stability check have been successfully proved, and optimal parameters gain values are listed in Table 2. The speed loop of the PMSM drive with total disturbance estimation based on the FTSMO is shown in Fig. 3.

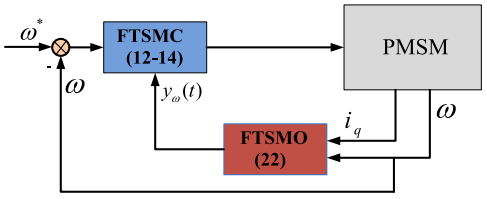

FIGURE 3. Block diagram of the proposed control method for the speed loop.

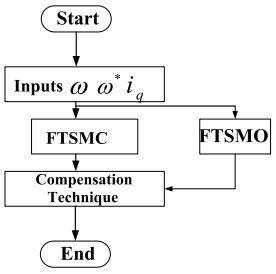

FIGURE 4. The flow diagram of the speed loop based on the improved FTSMO with FTSMC.

The dynamic speed response of the PMSM can be improved by using the FTSMO. Furthermore, it is very important to make correct selection on ℓ, otherwise, some chattering would occur in the drive system. The flow diagram of speed loop based on the FTSMO with FTSMC is depicted in Fig. 4.

D. STABILITY CHECK OF THE PROPOSED SLIDING TRAJECTORY

In this work, one second order system is considered by

$$\ddot{x}(t) = f(x_1, t) + bu(t) + y_d(t) \tag{29}$$

where $u(t)$ represents the control input, $y_d(t)$ the disturbance, and b the known gain. Hence, $f = -25\dot{x}$, $b = 133$, $y_d(t) = 10\sin(\pi t)$, and the signal $x_a = \sin t$ are chosen as the position reference with the initial state value $[-1.5, 1.5]$.

The conventional sliding surface is chosen as

$$s = x_2 + cx_1 \tag{30}$$

where $x_2 = \dot{x}_1$, c is the co-efficient of the x_1, which must satisfy the Hurwitz condition $c > 0$, and x_1 and x_2 are the tracking error and derivative of the CSMC, respectively. The FTSMC surface is decided by

$$s = x_2 + \lambda_1 |x_2|^{\alpha_1} + \lambda_2 |x_1|^{\alpha 2} \tag{31}$$

where λ_1 and λ_2 are the positive constants. In the Numerical Analysis Section, the parameter values of the sliding mode surface of CSMC and FTSMC for fair comparison are given in Table 1, which can be obtained through the Trial and Error method.

Moreover, The selction in the surface gains of the sliding mode control are very important to this work. The gain values of the c and $\lambda 2$ for the CSMC and FTSMC are propoerly tunned through the Trial and Error method, which is finally

TABLE 1. The slsinding mode suface and reaching law gain values for the CSMC and FTSMC for the numerical anlysis.

Parameters	Values and Units
The sliding mode surface and reaching law gains for CSMC	$C = 15$
The sliding mode surface and reaching law gains for FTSMC	λ_1= 60 and λ_2=15

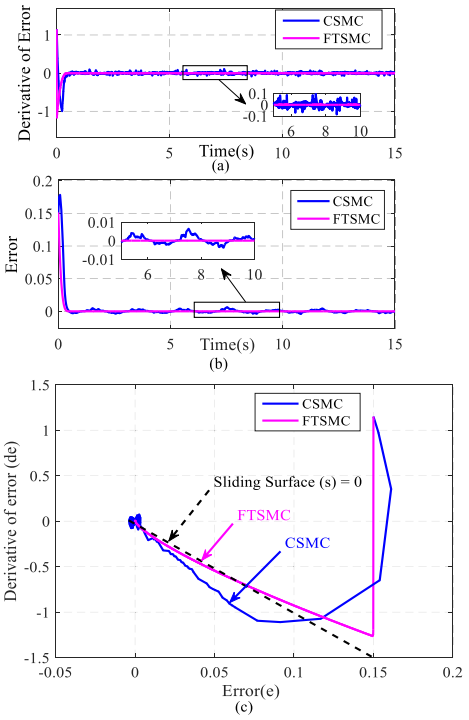

FIGURE 5. The responses of sliding surface for CSMC and FTSMC. (a) Derivative of the error. (b) Error under CSMC and FTSMC. (c) System phase trajectory.

tuned as 15, respectively. Thereof, if the gain values of c or λ2 are increased than 15, the overshoot would come out in the response of the position and speed signals, and vice versa. Therefore, the gain of 15 is optimal value for the c or λ2, respectively.

The stability checks on two sliding mode surfaces, CSMC and FTSMC, has been fully made by simulation, as illustrated in Figs. 5 and 6 respectively. Both Fig. 5(a) and Fig. 5(b) are considered to check the convergence rate and transient responses of the CSMC and CFTSMC sliding surfaces.

Moreover, Fig. 5 (a) shows the derivative of error responses under the CSMC and FTSMC. It is seen from this figure that the CSMC surface has greater steady state fluctuation, higher ripple, and bigger chattering than the FTSMC. Furthermore, it can be observed from Fig. 5(b) that the FTSMC response of sliding state is faster and smoother than that of CSMC. Fig. 6 shows the position and angular speed tracking responses under the CSMC and FTSMC. It is seen clearly from this figure that the FTSMC has stronger tracking capability than that of the CSMC, and the FTSMC has very small tracking error in the position, while the CSMC has 10% error in the position.

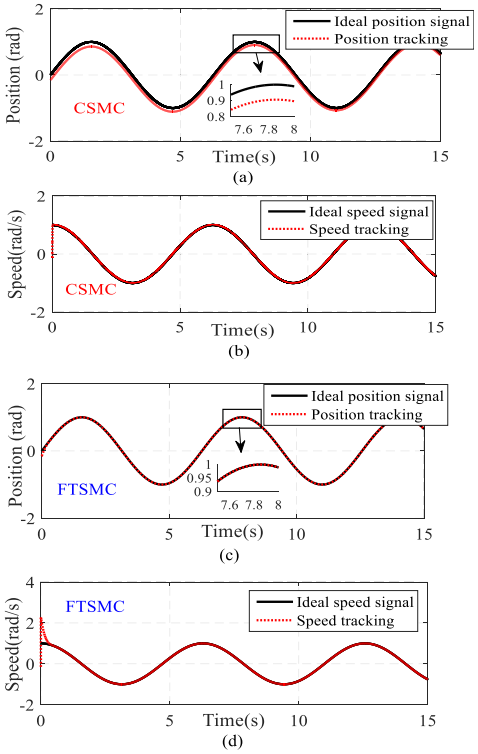

FIGURE 6. The tracking responses of the position and angular speed for CSMC and FTSMC. (a) Position under CSMC. (b) Angular speed under CSMC. (c) Position under FTSMC. (d) Angular speed under FTSMC.

TABLE 2. Nominalparameters of the PMSM.

Symbol	Parameters	Value and Unit
n_p	Pole pairs	3
p	Rated power	3.0 kW
R_s	Stator resistance	0.8 Ω
ψ_f	Flux linkage	0.35 Wb
L_s	Mutual inductance	0.005 H
J	Inertia	$3.78\times10^{-4} kg.m^2$
B	Viscous damping	1.74×10^{-5} N·m·s / rad

V. EXPERIMENTAL VALIDATION

In order to investigate the advantages of the FTSMO based on the FTSMC method, comprehensive experiments have been made in this section, which are fully compared with those of the conventional PI, CSMC and FTSMC, respectively. Main parameters for the control methods are given out in Table 2. The conventional sliding mode manifold for the CSMC has been chosen as

$$\vartheta = \dot{\mathrm{E}} + \alpha \mathrm{E} \tag{32}$$

Hence, the CSMC is designed as

$$i_q^* = F_t^{-1}(\dot{\omega}^* + \alpha \mathrm{E} + \int \lambda_1(\vartheta) + \lambda_2 |\vartheta|^{\delta_3} sign(\vartheta) dt) \tag{33}$$

where α, λ_1, and λ_2 are the control and switching gains of the CSMC, which are 4000, 0.001, and 20000, respectively.

In this work, one prototype for the PMSM drive system is built up, as illustrated in Fig. 7. An incremental encoder and

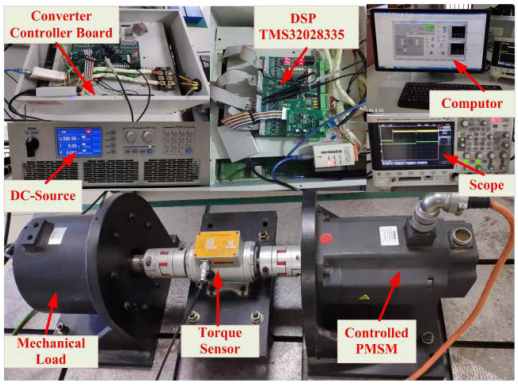

FIGURE 7. The test platform.

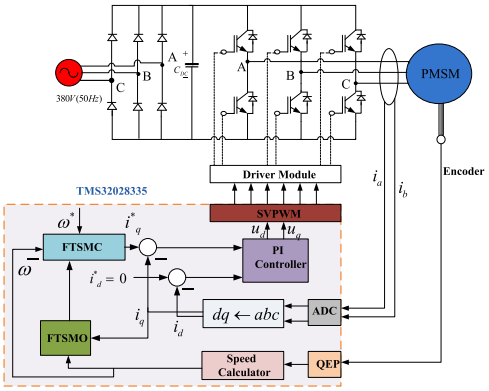

FIGURE 8. The circuit diagram of proposed control method.

TABLE 3. Specifications of the controller.

Parameters	Values and Units
PI gains for current controller	1 and 350
Sampling frequency	10 kHz
The gains of CSMC	$\alpha = 4000$ λ_1=0.001, and λ_2=200000
The gains of FTSMC	μ_1=4000, μ2=4000, λ1=0.001, and λ_2=100000
The gains of FTSMC+FTSMO	μ_1=4000, μ_2=4000, k_1=0.001, k_2 =80000, k=120, $\gamma_0 = 3$, $\gamma_1 = 1.5$, and $\gamma_2 = 1.2$

a hall current sensor are used to measure the rotating speed and the primary current, respectively. The load is managed by another PMSM coupled to the shaft of the originally controlled motor.

Moreover, the whole PMSM drive system based on the proposed method is shown in Fig. 8. Comprehensive experiments are made and fully compared with conventional PI, CSMC and FTSMC in different working conditions, including no-load, loaded and speed reverse conditions, respectively.

The full algorithm includes the SVPWM as implemented by the DSP-coding on the DSP (TMS32028335) controller. The control parameters for current and speed controllers of PI, CSMC, FTSMC, and FTSMO based FTSMC are designed, as listed in Table 3.

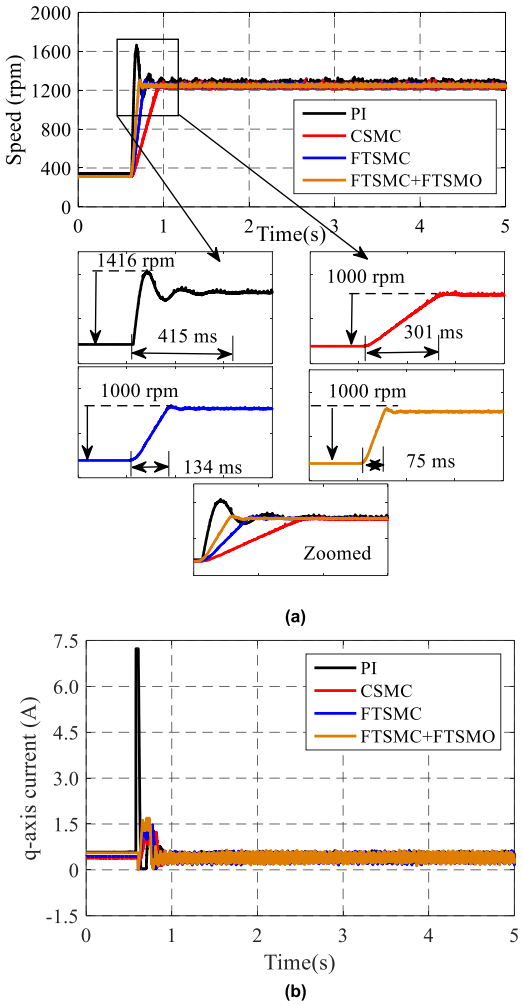

FIGURE 9. The no-load performances of the speed and q-axis current the PI, CSMC, FTSMC, and FTSMO based FTSMC methods under no-load with 1000 rpm. (a) Speed. (b) q-axis current.

Furthermore, the tunning of all variables for the CSMC, FTSMC and proposed FTSMO based FTSMC are dependent closely on the tuning process similar to the tuning of the PI controller. In this paper, these variables are obtained by adopting the Trial-and-Error Method so as to get better convergence, quicker tracking and stronger robustness against the load disturbances. The comparative tuned parameters have been already available in Table 2.

Case-1: (The Startup Transient and Steady State Performance under No-load Condition): In this case, the system performance is tested under no load. Simultaneously, the speed curves of the system under PI, CSMC, FTSMC, and FTSMO based FTSMC are shown in Fig.9 (a) and (b), and Fig.10 (a) and (b) with reference speed of 1000 rpm and 1600 rpm, respectively.

It is observed from these pictures that the actual speed response under the FTSMO based FTSMC can follow the desired speed very well in term of the quickest response, which means the speed response under proposed method can reach the steady-state in much shorter time than PI,

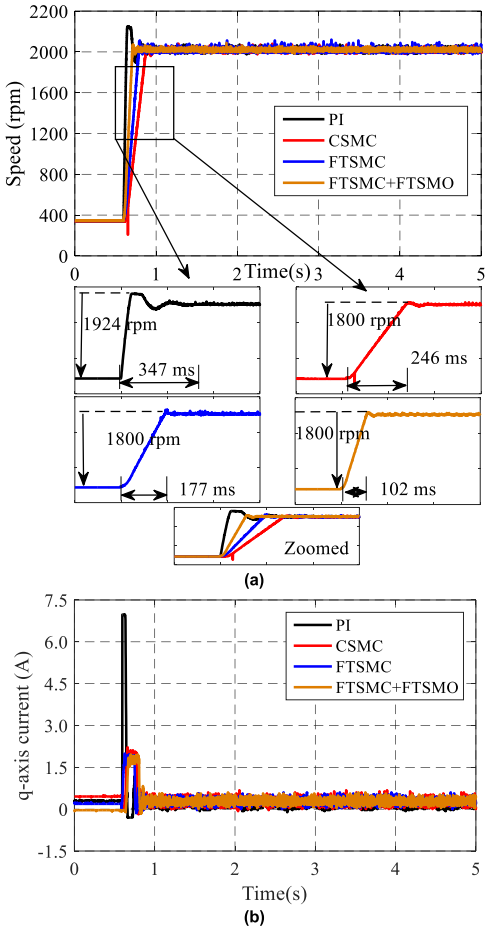

FIGURE 10. The no-load performances of the speed and q-axis current for the PI, CSMC, FTSMC, and FTSMO based FTSMC methods under no-load with 1600 rpm. (a) Speed. (b) q-axis current.

CSMC and FTSMC, separately. The settling times of speed response under PI, CSMC, FTSMC, and FTSMO based FTSMC with the reference speed of 1000 rpm and 1600 rpm are (415ms, 347ms), (301ms, 246ms), (134ms, 177ms), and (75ms, 102ms), separately. Because the SMC controller has the property of fast convergence, the CSMC, FTSMC, and FTSMO based FTSMC are observed faster in the startup transient than that of PI controller, respectively.

As seen from Figs.9 and 10, it is known that the PI controller has an overshoot during the start-up process under no-load condition, which seldom occurs in the CSMC, FTSMC, and FTSMO based FTSMC due to the SMC excellent control ability.

Specifically, it is observed from Fig. 9 (a) and 10 (a) that the FTSMO based FTSMC has smaller speed fluctuations in the steady state condition than that of PI, CSMC, and FTSMC, respectively. Moreover, from Fig.9 (b) and 10 (b), it is known that the q-axis current ripple and chattering under the FTSMO based FTSMC are smaller than PI, CSMC, and FTSMC during the start-up and steady states, separately.

Furthermore, the quantitative analysis has been added to make the paper very comprehensive for the readers under different indicators, which are listed in Tables 3 and 4,

TABLE 4. Start-up transient indexes of PI, CSMC, FTSMC AND FTSMC+FTSMO under reference Speed of 1000rpm and 1600 rpm.

Control method	Settling time (ms)		Steady-state error (± rpm)	
PI	415	347	30	50
CSMC	301	246	20	55
FTSMC	134	177	18	60
FTSMC+FTSMO	75	102	15	45

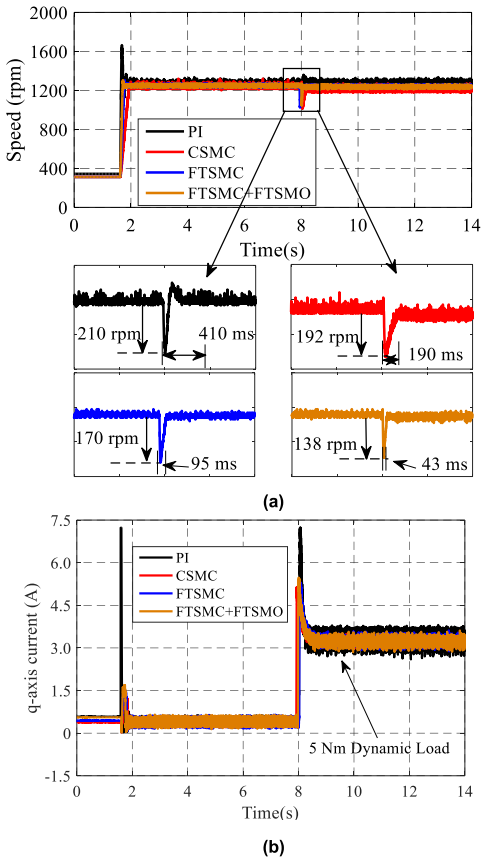

FIGURE 11. The anti-disturbance behavior of the speed and q-axis current with the PI, CSMC, FTSMC, and FTSMO based FTSMC methods under 5 Nm load with 1000 rpm. (a) Speed. (b) q-axis current.

individually. The startup and steady-state performance indexes based on PI, CSMC, FTSMC and FTSMC+FTSMO are listed under the reference speed of 1000 rpm and 1600 rpm, respectively, as depicted in Table 4.

It can be noted from Table 4 that the FTSMO based FTSMC is 82 %, 75% and 44 % quicker than those of PI, CSMC and FTSMC, respectively.

Case-2: (Anti-disturbance Performance of the Drive System:) In this study, the FTSMO based FTSMC method is verified under 1000 and 1600 rpm with 5 and 10 Nm load, as shown in Figs.11 and 12, respectively. In addition, it is observed from same picture that the speed drop and settling time under PI, CSMC, FTSMC, and FTSMO based FTSMC with dynamic load of 5 Nm are (210rpm, 410ms), (192rpm, 190ms), (170rpm, 95ms) and (138 rpm, 43 ms), respectively. Furthermore, the q-axis current response is shown in Fig. 11(b) for the aforementioned control methods under

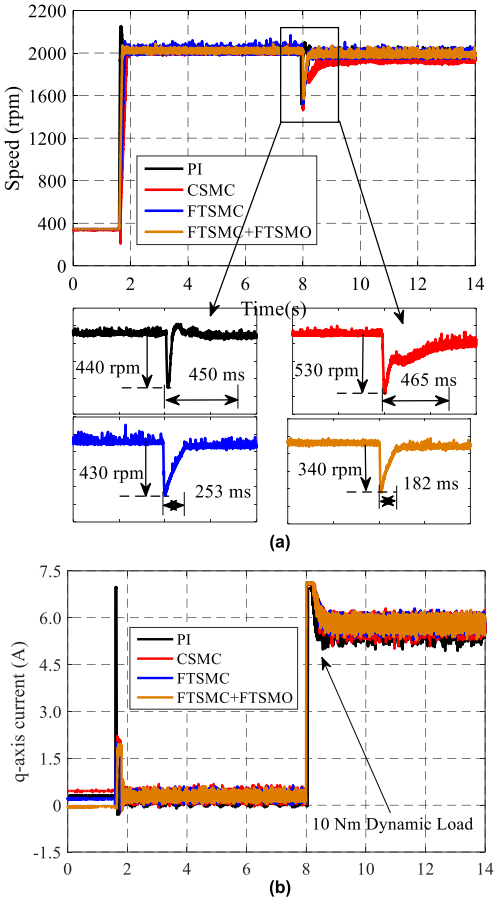

FIGURE 12. The anti-disturbance behavior of the speed and q-axis current with the PI, CSMC, FTSMC, and FTSMO based FTSMC methods under 10 Nm load with 1600 rpm. (a) Speed. (b) q-axis current.

TABLE 5. Anti-disturbance indexes of the PI, CSMC, FTSMC and FTSMC+FTSMO techniques.

Control Method	Speed drop (rpm) and reaching time(ms) with 5 Nm load		Speed drop (rpm) and reaching time time(ms) with 10 Nm load	
PI	210	410	440	450
CSMC	192	190	530	465
FTSMC	170	95	430	253
FTSMC+FTSMO	138	43	340	182

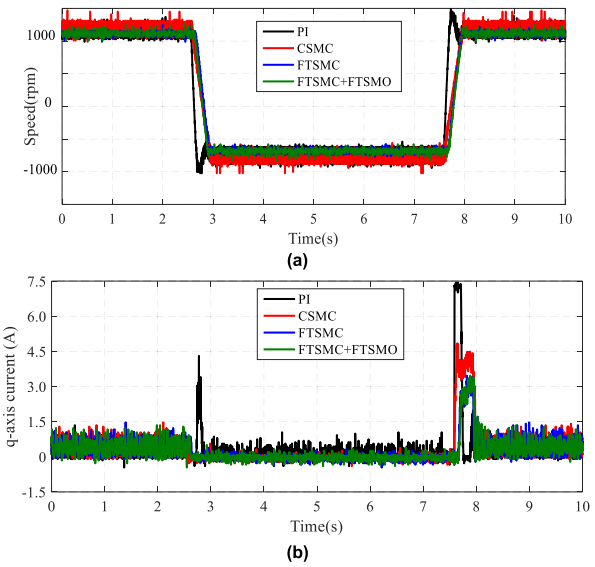

FIGURE 13. The speed reverse performances of the PMSM under the PI, CSMC, FTSMC, and FTSMO based FTSMC methods. (a) Speed. (b) q-axis current.

loaded condition, as observed from same picture that the FTSMO based FTSMC has smaller current ripple and chattering than PI, CSMC, and FTSMC, separately.

Again, the sudden 10 Nm load is added with the reference speed of 1600 rpm to validate the anti-disturbances property of the proposed method and fully compared with conventional PI, CSMC and FTSMC, respectively. It can be seen from Fig. 12 (b) that the FTSMO based FTSMC has quicker speed response than PI, CSMC and FTSMC, individually. The settling time is calculated as 450, 465, 253, 182 ms, and speed drop is observed as is 440, 530, 430, and 340 rpm under PI, CSMC, FTSMC, and FTSMO based FTSMC, individually. Furthermore, the q-axis current response is shown in Fig.12 (b) for the aforementioned control methods under the load of 10 Nm, where the FTSMO based FTSMC has smaller current ripple and chattering than PI, CSMC, and FTSMC, separately. It can be concluded that the proposed FTSMO based FTSMC has strong robust ability when the sliding state is near or far from the designed sliding mode surface.

Moreover, Table 5 has demonstrated much stronger robustness of the FTSMO based FTSMC against load disturbances than those of PI, CSMC and FTSMC under 5 Nm and 10 Nm, separately. Therefore, it is seen that Table 4 has confirmed that the proposed (FTSMC+FTSMO) method has superior performance against load disturbances and quicker transient response over PI, CSMC and FTSMC, respectively.

Case-3: (The Dynamics of the System under Speed Reversal Condition):

In this case, the speed reversal dynamic performance of PMSM drive system has been checked and compared under PI, CSMC, FTSMC, and FTSMO based FTSMC. The speed reversal process has been taken from 1000 to -1000 rpm and then -1000 to 1000 rpm, as shown in Fig. 13. It can be observed from the same picture that the speed response has an overshot under PI controller, and needs more time to settle on the steady state. At the same time, it is also seen from Fig. 13(a) that the speed under the FTSMO based FTSMC has faster response, stronger robust tracking ability, and smaller steady state error during the reversal operation than the PI, CSMC, and FTSMC, separately. As noted from Fig.13(b) that current ripple inherent chattering phenomenon are smaller than the conventional PI, CSMC and FTSMC, separately.

VI. CONCLUSION

In this paper, the FTSMO based FTSMC has been implemented for the speed regulation of the PMSM drive system

with load disturbance. Main contributions of this paper can be summarized as follows:

(1) One new FTSMC is introduced in this paper, which is designed and implemented to ensure the fast convergence in the finite time and alleviate the chattering effectively.

(2) One disturbance estimation strategy based on the FTSMO with the feed-forward compensation technique is proposed to eliminate the chattering phenomena effectively, which can enhance the whole drive system performance against the load disturbances.

(3) The Lyapunov theorem is employed to analyze the PMSM drive performance and stability of the FTSMC and FTSMO with FTSMC, respectively.

(4) The PMSM drive performance under FTSMO based FTSMC method has been fully compared with those of the conventional PI, CSMC and FTSMC, separately.

Both simulation and experimental results have fully demonstrated that the FTSMO based FTSMC method can get quicker dynamic response, stronger robustness under load and speed change, lower q-axis chattering in comparison to those of conventional PI, CSMC and FTSMC, individually.

Due to the excellent drive performance, the FTSMO based FTSMC in this work can be also employed for the PMSM current loops next step.

REFERENCES

[1] W. Tong, S. Dai, S. Wu, and R. Tang, "Performance comparison between an amorphous metal PMSM and a silicon steel PMSM," *IEEE Trans. Magn.*, vol. 55, no. 6, pp. 1–5, Jun. 2019.
[2] G.-J. Wang, C.-T. Fong, and K. J. Chang, "Neural-network-based self-tuning PI controller for precise motion control of PMAC motors," *IEEE Trans. Ind. Electron.*, vol. 48, no. 2, pp. 408–415, Apr. 2001.
[3] K.-H. Kim and M.-J. Youn, "A nonlinear speed control for a PM synchronous motor using a simple disturbance estimation technique," *IEEE Trans. Ind. Electron.*, vol. 49, no. 3, pp. 524–535, Jun. 2002.
[4] A. V. R. Teja, C. Chakraborty, and B. C. Pal, "Disturbance rejection analysis and FPGA-based implementation of a second-order sliding mode controller fed induction motor drive," *IEEE Trans. Energy Convers.*, vol. 33, no. 3, pp. 1453–1462, Sep. 2018.
[5] M. H. Holakooie, M. Ojaghi, and A. Taheri, "Modified DTC of a six-phase induction motor with a second-order sliding-mode MRAS-based speed estimator," *IEEE Trans. Power Electron.*, vol. 34, no. 1, pp. 600–611, Jan. 2019.
[6] L. Rui, M. Draga, and L. Leyva, "Second-order sliding-mode controlled synchronous buck DC–DC converter," *IEEE Trans. Power Electron.*, vol. 31, no. 3, pp. 1358–1365, Mar. 2016.
[7] M. Preindl and S. Bolognani, "Model predictive direct speed control with finite control set of PMSM drive systems," *IEEE Trans. Power Electron.*, vol. 28, no. 2, pp. 1007–1015, Feb. 2013.
[8] Z. Pan, F. Dong, J. Zhao, L. Wang, H. Wang, and Y. Feng, "Combined resonant controller and two-degree-of-freedom PID controller for PMSLM current harmonics suppression," *IEEE Trans. Ind. Electron.*, vol. 65, no. 9, pp. 7558–7568, Sep. 2018.
[9] Y. Yi, D. M. Vilathgamuwa, and M. A. Rahman, "Implementation of an artificial-neural-network-based real-time adaptive controller for an interior permanent-magnet motor drive," *IEEE Trans. Ind. Appl.*, vol. 39, no. 1, pp. 96–104, Jan. 2003.
[10] Y. S. Kung and M. H. Tsai, "FPGA-based speed control IC for PMSM drive with adaptive fuzzy control," *IEEE Trans. Power Electron.*, vol. 22, no. 6, pp. 2476–2486, Nov. 2007.
[11] X. Zhang, L. Sun, K. Zhao, and L. Sun, "Nonlinear speed control for PMSM system using sliding-mode control and disturbance compensation techniques," *IEEE Trans. Power Electron.*, vol. 28, no. 3, pp. 1358–1365, Mar. 2013.
[12] W. Xu, A. Junejo, Y. Liu, and R. Islam, "Improved continuous fast terminal sliding mode control with extended state observer for speed regulation of PMSM drive system," *IEEE Trans. Veh. Technol.*, vol. 68, no. 11, pp. 10465–10476, Nov. 2019.
[13] K. Ma, "Comments on 'quasi-continuous higher order sliding-mode controllers for spacecraft-attitude-tracking maneuvers,'" *IEEE Trans. Ind. Electron.*, vol. 60, no. 7, pp. 2771–2773, Jul. 2013.
[14] E. Cruz-Zavala and J. A. Moreno, "Higher order sliding mode control using discontinuous integral action," *IEEE Trans. Autom. Control*, vol. 65, no. 10, pp. 4316–4323, Oct. 2020.
[15] H. Hou, X. Yu, L. Xu, K. Rsetam, and Z. Cao, "Finite-time continuous terminal sliding mode control of servo motor systems," *IEEE Trans. Ind. Electron.*, vol. 67, no. 7, pp. 5647–5656, Jul. 2020.
[16] J. Zhang, H. Wang, J. Zheng, Z. Cao, Z. Man, M. Yu, and L. Chen, "Adaptive sliding mode-based lateral stability control of steer-by-wire vehicles with experimental validations," *IEEE Trans. Veh. Technol.*, vol. 69, no. 9, pp. 9589–9600, Sep. 2020.
[17] G. Guo and D. Li, "Adaptive sliding mode control of vehicular platoons with prescribed tracking performance," *IEEE Trans. Veh. Technol.*, vol. 68, no. 8, pp. 7511–7520, Aug. 2019.
[18] Y. Feng, X. Yu, and F. Han, "High-order terminal sliding-mode observer for parameter estimation of a permanent-magnet synchronous motor," *IEEE Trans. Ind. Electron.*, vol. 60, no. 10, pp. 4272–4280, Oct. 2013.
[19] X. Yu and Z. Man, "Fast terminal sliding-mode control design for nonlinear dynamical systems," *IEEE Trans. Circuits Syst.*, vol. 49, no. 2, pp. 261–264, Feb. 2002.
[20] L. Yang and J. Yang, "Nonsingular fast terminal sliding-mode control for nonlinear dynamical systems," *Int. J. Robust Nonlinear Control*, vol. 21, no. 16, pp. 1865–1879, Nov. 2011.
[21] W. Xu, R. Dian, Y. Liu, D. Hu, and J. Zhu, "Robust flux estimation method for linear induction motors based on improved extended state observers," *IEEE Trans. Power Electron.*, vol. 34, no. 5, pp. 4628–4640, May 2019.
[22] S. S. D. Xu, C. C. Chen, and Z. L. Wu, "Study of nonsingular fast terminal sliding-mode fault-tolerant control," *IEEE Trans. Ind. Electron.*, vol. 62, no. 6, pp. 3906–3913, Jun. 2015.
[23] W. Xu, A. K. Junejo, Y. Liu, M. G. Hussien, and J. Zhu, "An efficient antidisturbance sliding-mode speed control method for PMSM drive systems," *IEEE Trans. Power Electron.*, vol. 36, no. 6, pp. 6879–6891, Jun. 2021.
[24] M. Ismail, W. Xu, X. Wang, A. Junejo, Y. Liu, and M. Dong, "Analysis and optimization of torque ripple reduction strategy of surface-mounted permanent-magnet motors in flux-weakening region based on genetic algorithm," *IEEE Trans. Ind. Appl.*, vol. 57, no. 4, pp. 4091–4106, Jul. 2021.
[25] R. Miranda-Colorado, "Robust observer-based anti-swing control of 2D-crane systems with load hoisting-lowering," *Nonlinear Dyn.*, vol. 104, no. 1, pp. 3581–3596, Apr. 2021.

WEI XU (Senior Member, IEEE) received the B.E. and M.E. degrees in electrical engineering from Tianjin University, Tianjin, China, in 2002 and 2005, respectively, and the Ph.D. degree in electrical engineering from the Institute of Electrical Engineering, Chinese Academy of Sciences, in 2008.

From 2008 to 2012, he was a Postdoctoral Fellow with the University of Technology Sydney, a Vice Chancellor Research Fellow with the Royal Melbourne Institute of Technology, and a Japan Science Promotion Society Invitation Fellow with Meiji University. Since 2013, he has been a Full Professor with the State Key Laboratory of Advanced Electromagnetic Engineering, Huazhong University of Science and Technology, China. He has more than 110 articles accepted or published in IEEE journals, two edited books published by Springer Press, one monograph published by China Machine Press, and more than 150 invention patents granted or in pending, all in the related fields of electrical machines and drives. His research interest includes design and control of linear/rotary machines. He is a fellow of the Institute of Engineering and Technology (IET). He is the General Chair for 2021 International Symposium on Linear Drives for Industry Applications (LDIA 2021) and 2023 IEEE International Conference on Predictive Control of Electrical Drives and Power Electronics (PRECEDE 2023), Wuhan, China. He has served as an Associate Editor for several leading IEEE TRANSACTIONS and journals, such as the IEEE TRANSACTIONS ON INDUSTRIAL ELECTRONICS, the IEEE TRANSACTIONS ON VEHICULAR TECHNOLOGY, and the IEEE TRANSACTIONS ON ENERGY CONVERSION.

ABDUL KHALIQUE JUNEJO was born in Larkana, Sindh, Pakistan, in 1989. He received the bachelor's and master's degrees in electrical engineering from Quaid-e-Awam UEST, Nawabshah, Sindh, in 2011 and 2015, respectively, and the Ph.D. degree from the State Key Laboratory of Advanced Electromagnetic Engineering, School of Electrical and Electronics Engineering, Huazhong University of Science and Technology, Wuhan, China. He is currently employed as an Assistant Professor with Quaid-e-Awam UEST. His research interests include the sliding mode control, direct torque control (DTC), model predictive control (MPC) and sensorless control methods for permanent magnet synchronous machines (PMSM), and induction machines (IM) and Linear IM and drives. He has served as a Reviewer for IEEE journals, including the IEEE TRANSACTIONS ON INDUSTRIAL ELECTRONICS, the IEEE TRANSACTIONS ON POWER ELECTRONICS, the IEEE TRANSACTIONS ON TRANSPORTATION ELECTRIFICATION, *Assembly Automation* (Emerald Group Publishing Ltd.), Article in Journal, and IEEE JOURNAL OF EMERGING AND SELECTED TOPICS IN INDUSTRIAL ELECTRONICS.

YIRONG TANG (Student Member, IEEE) received the B.E. degree in electrical engineering from the Huazhong University of Science and Technology, Wuhan, China, in 2020, where he is currently pursuing the Ph.D. degree with the State Key Laboratory of Advanced Electromagnetic Engineering and Technology.

His research interests include advanced control methods for permanent magnet synchronous machines (PMSM), and linear induction machines (LIM) and drives.

MUHAMMAD SHAHAB received the B.Sc. degree in electrical engineering from the FAST, National University of Computer and Emerging Science (NUCES), Pakistan, in 2013, and the dual M.Sc. degree in new energy science and engineering from the Huazhong University of Science and Technology (HUST), Wuhan, China, and MINES Paris Tech France, in 2016. He is currently pursuing the Ph.D. degree in electrical engineering with the HUST. His research interests include distributed generation control, power quality improvements, power and energy consumption analysis using machine learning, and smart power electronics-controlled inverters in smart microgrids. He is a member of Pakistan Engineering Council (PEC).

HABIB UR RAHMAN HABIB (Graduate Student Member, IEEE) was born in Fort Abbas, Pakistan. He received the B.Sc. degree in electrical engineering and the M.Sc. degree in electrical power engineering from the University of Engineering and Technology Taxila, Pakistan, in 2009 and 2015, respectively. He is currently pursuing the Ph.D. degree with the State Key Laboratory of Advanced Electromagnetic Engineering and Technology, Huazhong University of Science and Technology, Wuhan, China. Since 2009, he has been with the COMSATS Institute of Information Technology, Pakistan, and the Wah Engineering College, University of Wah, Pakistan. He has been a Management Trainee Officer (Maintenance Department) with Dynamic Packaging Pvt. Ltd., Lahore, Pakistan. He is also permanently with the Department of Electrical Engineering, University of Engineering and Technology Taxila. His research interests include renewable energy (RE), microgrids (MGs), model predictive control (MPC) and its applications in power industry, electrical planning and estimation, energy resources and planning, modeling and simulation, renewable energy technology and management, smart grid applications in power systems, distributed generation and ac/dc microgrids, power electronics, power quality issues, artificial intelligence, deep learning, machine learning, blockchain, fuzzy controllers, heuristic algorithms design and optimization, energy economics, automated microgrid and distribution systems, the smart IoT, green/smart buildings, building-integrated photovoltaics, environmental efficiency, energy security, and energy and sustainable development.

YI LIU (Senior Member, IEEE) received the B.E. and M.E. degrees in automation and control engineering from the Wuhan University of Science and Technology, Wuhan, China, in 2004 and 2007, respectively, and the Ph.D. degree in mechatronic engineering from the Huazhong University of Science and Technology, Wuhan, in 2016.

From March 2016 to June 2016, he was a Senior Research and Development Engineer with the Fourth Academy of China Aerospace Science and Industry Group, Wuhan. From July 2016 to October 2019, he was a Postdoctoral Research Fellow at the State Key Laboratory of Advanced Electromagnetic Engineering and Technology, Huazhong University of Science and Technology, where he has been a Lecturer, since January 2020. His current research interests include multi-port electrical machines and drive systems. He has received one IEEE Prize Paper Award in 2020. He is the Vice Chair of the IEEE IES Wuhan Chapter and an Associate Editor of the IEEE TRANSACTIONS ON INDUSTRY APPLICATIONS.

SHOUDAO HUANG (Senior Member, IEEE) was born in Hunan, China, in 1962. He received the B.S. and Ph.D. degrees in electrical engineering from the College of Electrical and Information Engineering, Hunan University, Changsha, China, in 1983, and 2005, respectively.

He is currently a full-time Professor with the College of Electrical and Information Engineering, Hunan University. His research interests include motor design and control, power electronic system and control, and wind energy conversion systems.